

THE STATUS OF THE SLAC LINEAR COLLIDER AND OF THE MARK II DETECTOR^{*)}

A. J. Lankford

Stanford Linear Accelerator Center, Stanford University, Stanford, CA 94305

INTRODUCTION

At SLAC we are currently involved in the exciting challenge of commissioning the first example of a new type of colliding beam accelerator, the SLAC Linear Collider, or SLC. The goals of the SLC are two-fold. It will explore the concept of linear colliders, and it will allow the study of physics on the Z^0 resonance. It accomplishes these goals by exploiting the existing SLAC linac and the large visible cross-section of approximately thirty nanobarns of the Z^0 . The MARK II detector will have the opportunity to be first to explore the physics in this regime.

This paper briefly reports the status of the SLC and of the MARK II as of early October 1987, at which time commissioning efforts were interrupted in order to place the MARK II detector at the collision point and to incorporate some improvements to the SLC. The first portion of this report highlights some of the milestones achieved in the SLC commissioning and some of the problems encountered. The last portion outlines improvements made to the MARK II for physics at the SLC.

OVERVIEW OF THE SLC

Linear colliders have been proposed as a cost-effective means of providing e^+e^- collisions at higher energies than LEP-generation storage rings. Whereas, storage rings suffer limitations due to energy loss via synchrotron radiation, linear colliders produce synchrotron radiation only as "beamstrahlung" in the intense fields of the colliding beams. In addition, since the beams do not need to be recollided after collision, linear colliders can produce extremely intense collisions of high-density, small beams in which "disruptive" effects actually enhance luminosity rather than diminish it. Expressed in terms of parameters at the interaction point, the luminosity is:

$$\mathcal{L} = \frac{N^+ N^-}{4\pi\sigma^2} f H$$

where N^+ and N^- are the number of particles in the colliding bunches of positrons and electrons, σ is the RMS beam radius, f is the frequency of collision, or repetition rate, and H is the enhancement factor which represents the increase

^{*)}Work supported by the Department of Energy, contract DE-AC03-76SF00515.

in luminosity due to the focussing of the beams in the fields of each other. Of course, the beam radius at the interaction point depends on other parameters, such as emittance and bunch length.

The SLC achieves the effect of colliding linacs by using the existing SLAC linac to simultaneously accelerate both positron and electron beams and transporting the beams through two "arcs" to collide head-on at the interaction point. Figure 1 shows the overall layout of the SLC. Two bunches of electrons are produced by an electron source consisting of a gated thermionic gun and a bunch compression system. The electrons are then accelerated from 160 keV to 200 MeV by a linear accelerator. The two electron bunches are joined by a 200 MeV positron bunch produced in the positron source. The three bunches are accelerated to 1.2 GeV by another linac. A splitter magnet separates the electron bunches and the positron bunch and sends them towards their respective damping rings. The transverse emittance of the bunches is damped by synchrotron radiation in the rings. The electron bunches are damped for the interval between linac cycles, 8.3 msec for 120 Hz operation. The positron bunch is damped for two linac cycles, there being always two positron bunches stored in the ring. The two bunches of electrons and one bunch of positrons are extracted into transport lines between the damping rings and the linac which contain bunch compression systems. These systems employ a section of powered waveguide to introduce a correlation between particle position along the bunch and particle energy, which because of the non-isochronous beam transport reduces the bunch length. In the linac, the positron bunch precedes the electron bunches. The three bunches are accelerated together, separated by 59 nanoseconds. The positron bunch and the first electron bunch are accelerated to 47 GeV for 92 GeV in the center-of-mass at the collision point. Positrons and electrons are separated at the end of the linac into two high-gradient beam transport systems, referred to as "arcs", which are achromatic to second order. Approximately 1 GeV in beam energy is lost to synchrotron radiation in the arcs. The arcs transport the two beams to a final focus optical system which, after optical matching, focuses the beams to the smallest spot size necessary for luminosity and brings the beams into collision. The two beams are then extracted to dumps. The second electron bunch is used to produce positrons. It is extracted at 33 GeV, at the 2/3 point of the linac, and collided with a target. Positrons produced in the target are captured by a solenoidal focusing system and a very high-gradient accelerating section. They are accelerated to 200 MeV and returned along the length of the linac in a special return line to the point at which they are injected into the linac, accelerated to 1.2 GeV, and stored in the positron damping ring.

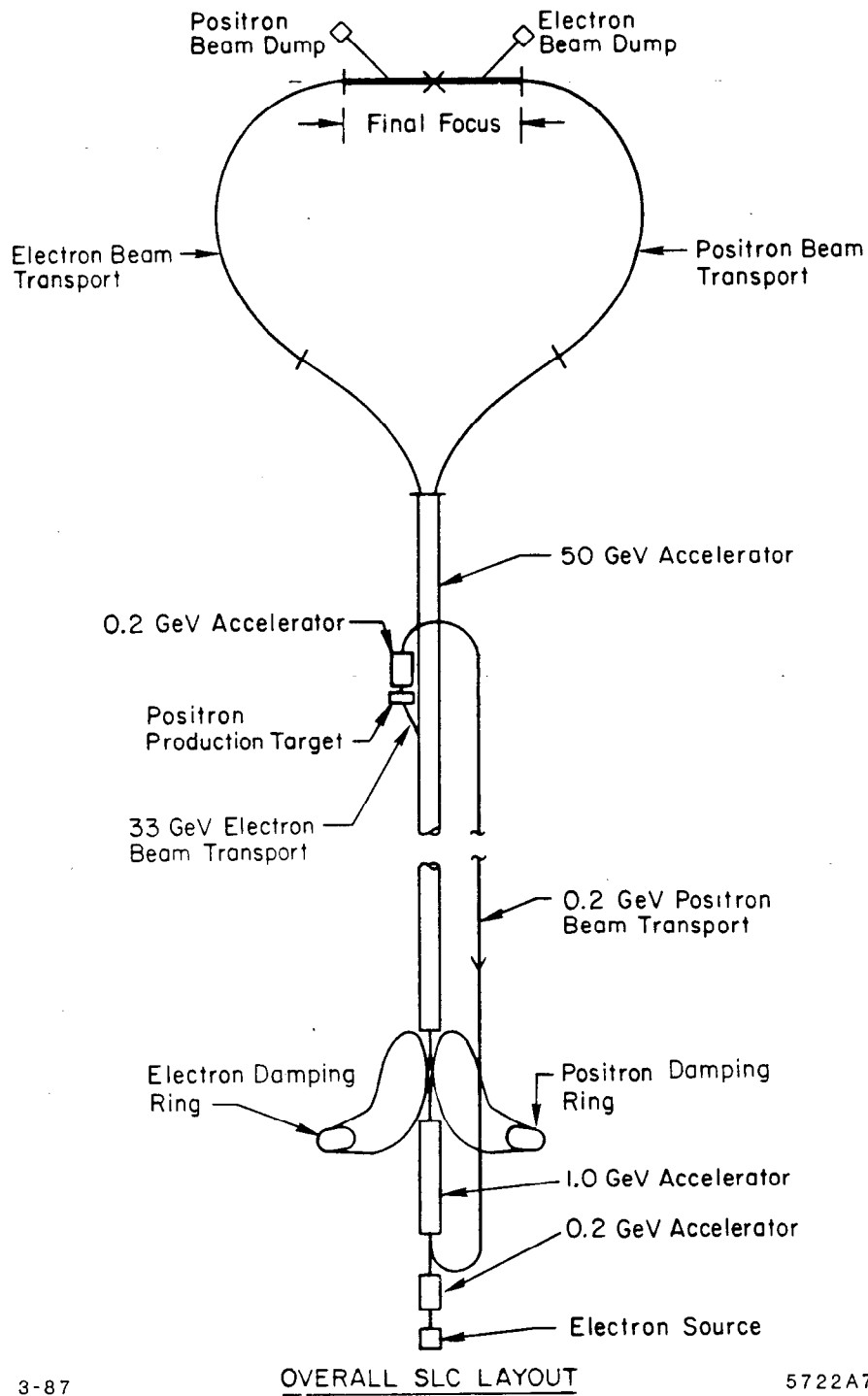


Fig. 1. Schematic of the overall layout of the SLC.

— Important design parameters of the SLC are shown in Table I, along with values of these parameters set as initial goals for the physics program. The values of these parameters achieved to date, also shown in Table I, are discussed below along with the status of the SLC.

Table I. Basic Parameters of the SLC

	Design Goal	Initial Goal	Achieved	Units
Beam Energy at IP	50	46	46	GeV
Beam Energy at End of Linac	51	47	53	GeV
Electrons at Entrance of Arcs	7×10^{10}	1×10^{10}	2.5×10^{10}	
Positrons at Entrance of Arcs	7×10^{10}	1×10^{10}	0.6×10^{10}	
Repetition Rate	180	60	5	Hz
Bunch Length σ_s	1.5	1.5	1.5	mm
Transverse Emittance at End of Linac	3×10^{-5}	5×10^{-5}	$3-20 \times 10^{-5}$	mrad
Spot Radius at IP	1.6	2.8	~ 6	Microns
Luminosity	6×10^{30}	6×10^{27}	—	$\text{cm}^{-2} \text{sec}^{-1}$
Z ⁰ 's per day	1.5×10^4	15	—	

STATUS OF THE SLC

Electron Source and Injector

For design luminosity the electron source and injector must provide two bunches of 7×10^{10} electrons with a momentum spread within the damping ring acceptance of $\pm 1\%$. The emittance requirement depends upon the period available for damping in the rings, and hence on the repetition rate. For 180 Hz operation, the transverse emittance spread must be less than 30×10^{-5} mrad; whereas, at 120 Hz it can be as great as 180×10^{-5} mrad. The emittance requirement for 120 Hz operation and the momentum spread requirement are met without difficulty with bunch populations of 5×10^{10} electrons. The emittance requirement for 180 Hz operation has not been consistently met with bunch populations greater than 4×10^{10} electrons. For future polarized beams, the thermionic gun will be replaced by a source which produces longitudinally polarized electrons by irradiating a GaAs crystal with circularly polarized light.

Damping Rings

The damping rings must damp the transverse emittance of the beams to the design value of 3.0×10^{-5} mrad within the period between linac pulses. At 120 Hz, 8.3 msec are available for damping. In the electron ring, two bunches must be damped simultaneously, as well as injected into and extracted from orbits separated by half the circumference of the ring. In addition, the length of bunches of electrons and positrons must be shortened to 1.5 mm between extraction and reinjection to the linac. The maximum bunch length acceptable is determined by energy spread and wakefield effects during acceleration in the linac.

Initial commissioning of both rings is complete. Transverse emittance requirements for operation at 120 Hz are readily achieved during available damping time, as shown in Fig. 2. In order to reach the damping times required for 180 Hz operation, it would be necessary to couple vertical and horizontal betatron motion to decrease the horizontal emittance with an acceptable increase in vertical emittance.

Following the installation of a redesigned kicker magnet, two electron bunches separated by 59 nsec have been simultaneously injected into the electron ring. During the present Autumn 1987 shutdown a new extraction kicker will be installed, which will permit simultaneous extraction of the two bunches, and hence, operation at 120 Hz. Without successful injection and extraction of two electron bunches, operation would be limited to 60 Hz, where alternate linac cycles at 120 Hz accelerate bunches of electrons for production of positrons and for transport to the interaction point.

The bunch length in the damping ring has a dependence on the bunch population which was not anticipated. The design bunch length in the ring is 6 mm. The dependence on current, illustrated in Fig. 3, is caused by excessive longitudinal impedance of the vacuum chamber in the ring. The large impedance arises from the small vacuum pipe through the high field bending magnets and from many transitions in the vacuum chamber. Modifications to the compression system during the present Autumn 1987 shutdown are designed to allow compression of bunches larger than 3×10^{10} particles to the design value of 1.5 mm. Further modifications may be necessary for operation at design current.

Linac

For SLC operation, the linac must simultaneously accelerate both electron and positron beams to the energies needed for Z^0 production, while delivering an additional electron bunch to the positron target. The beams must be delivered

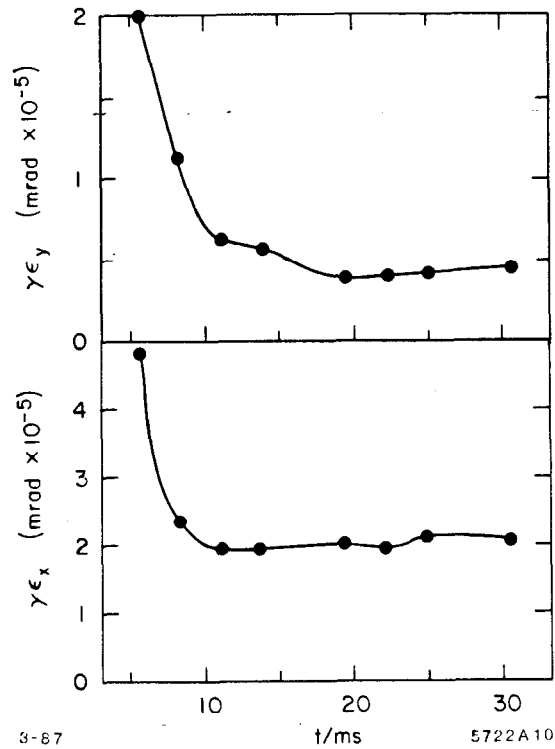


Fig. 2. Invariant emittance of beam extracted from the damping ring as a function of time after injection into the ring.

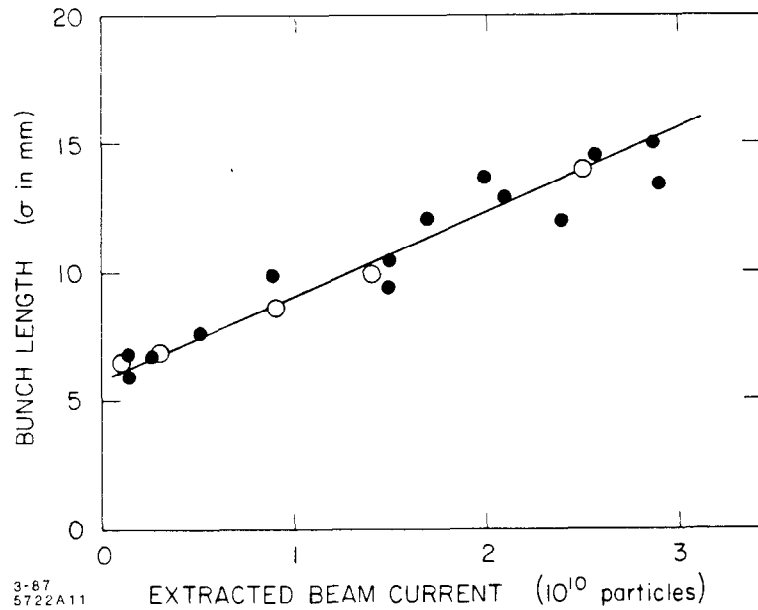


Fig. 3. Bunch length in the damping ring as a function of bunch population.

without significantly increasing their emittances and with a total energy spread of $\pm 0.2\%$.

In order to reach Z^0 energies, newly designed 67 MW klystrons were installed. Problems in early versions, window breakage, cathode gas emission, and microwave instability, were solved. The linac is now equipped with sufficient new klystrons for operation to 53 GeV. Experience with respect to cathode lifetime has been encouraging, although most operation has been at 10 Hz. The lifetime is now projected to be greater than 40,000 hours, and the mean time between failures is now greater than 18,000 hours and is increasing. At present the linac cannot operate at greater than 120 Hz because of power limitations of the linac modulators.

Transverse wake fields, which arise from space charge effects in the accelerating structure, can displace the phase space of the trailing part of a bunch relative to the phase space of the leading part. This effect can cause transverse wakefield tails. The size of the effect depends on bunch current, bunch length, and the accuracy with which the beam is centered in the accelerating structure. The linac has been instrumented with a new control system designed to center the beam with an RMS error less than 100 microns. Feedback algorithms have been implemented to simultaneously steer both electron and positron beams. Typical operation currently gives RMS steering errors of about 200 microns for single beams, and of 270 microns for electrons and 500 microns for positrons when the beams are steered simultaneously. Figure 4 illustrates the effect of inaccurate steering on beam tails. Figure 4a shows a profile of a beam with a small wakefield tail; whereas, Fig. 4b shows the large wakefield tail of a poorly steered beam.

At intensities of 1×10^{10} particles, the horizontal emittance at the end of the linac currently is several times larger than the design value of 3×10^{-5} mrad; whereas the vertical emittance meets the design value. The increase in apparent emittance between exit from the damping ring and exit from the linac is believed to arise from residual dispersion in the ring-to-linac transport system. The emittance increases with intensity due primarily to the increased bunch length. At higher intensities, wake field effects may cause further increases in emittance. The increase in emittance between exit from the damping ring and exit from the linac is believed to arise from residual dispersion in the ring-to-linac transport system.

An energy feedback system maintains the beam energy within 0.1% of nominal. An RMS energy jitter of less than 0.13% has been achieved. The energy spread of the bunch currently meets the design value only for bunch intensities less than about 1×10^{10} . At higher intensities, the energy spread is limited by the increases in bunch length with bunch current (see Damping Rings). Increased energy spread leads to increased spot size at the interaction point, particularly for energy spreads greater than 0.5%. A fast feedback system using energy and energy spread data from each pulse is currently being implemented. Further feedback systems control

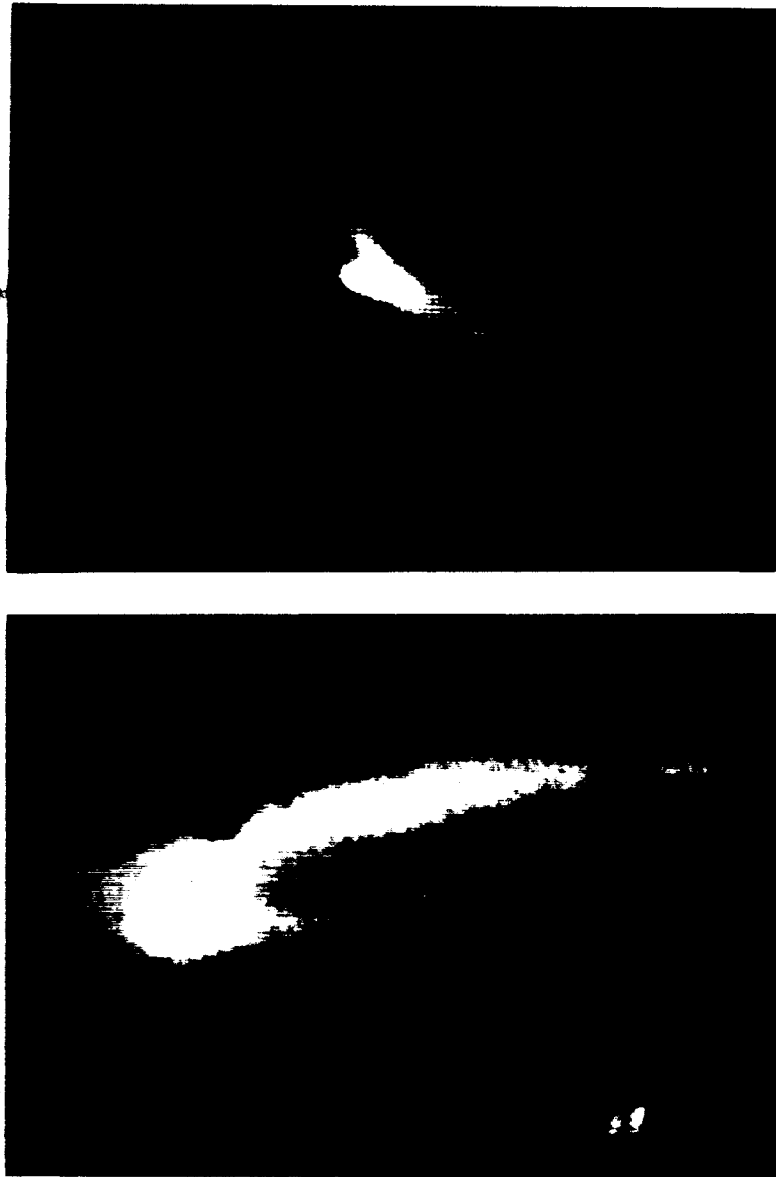


Fig. 4. Beam profile as seen by a phosphorescent screen at the end of the linac, (a) for a well-steered beam, and (b) for a poorly steered beam.

such functions as launch angles from the linac into the arcs. Refinement of the feedback algorithms continues.

Positron Source

The positron source must produce and return sufficient positrons to yield one positron in the linac for each electron incident on the positron target. Although this performance has nearly been achieved, routine operation is at roughly half this level. However, the focusing solenoid has been operating at reduced field, and the accelerating gradient in the high-gradient capture section has been operating at half its design value. These components, as well as a defective vacuum chamber are

being replaced during the current Autumn 1987 shutdown. With these changes, the positron yield is expected to double. Acceptance of positrons into the damping ring will also improve when the bunch compression systems are improved, since shorter incident electron bunch lengths will produce shorter positron bunch lengths at injection into the positron ring. An improved positron target is also planned for the future.

Arcs

The arcs are designed to transport the beams from the linac to the final focus with minimal emittance growth. This goal is accomplished by a very high-gradient transport system composed entirely of combined function magnets, whose profile is shown in Fig. 5. This design fixes the relative strengths of dipole, quadrupole, and sextupole moments. Consequently, the alignment of the magnets is crucial to achieving the proper orbit and for achromatic transmission of the beam. The design of the arcs incorporates mechanical magnet movers to adjust the position of the magnets according to orbit data. Random alignment errors in the electron arc are currently about 150 microns; whereas, the design calls for an RMS error of 100 microns. Systematic errors in the placement of the magnetic centers, originally found at the 200 to 400 micron level, have mostly been corrected

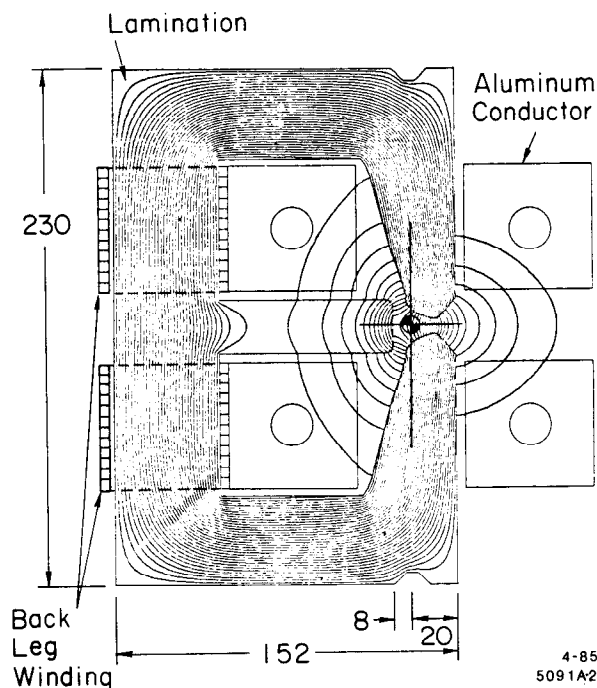


Fig. 5. Cross-section of the high-gradient combined function bending magnet used in the SLC arcs. The current-carrying conductors are perpendicular to the page. Physical dimensions in millimeters and magnetic flux distributions are shown.

by experimentally tuning the betatron phase advance in each achromat. The present alignment is adequate for achieving spot sizes at the final focus of about 3 microns. The present magnet mover design is being evaluated as to whether it allows reproducible accuracy of 100 microns.

Transmission through the arcs is very sensitive to phase shift errors through the lattice. The sensitivity arises because the arcs do not lie in a plane; instead they follow the local terrain. At each roll, that is, a point where the radius of curvature of the arc changes planes, cross-plane coupling occurs between the horizontal and vertical betatron oscillations. This coupling is reversed at the compensating roll, where the radius of curvature returns to the original plane; however, it is precisely reversed only if the total phase advance in both dimensions is a multiple of 2π between rolls. If cross-plane coupling remains, a mismatch in the β function occurs, possibly leading to transmission problems and to dispersion effects too large for correction by the optics of the final focus. The phase advance is difficult to measure directly; consequently, the phase advance has been systematically studied by giving the orbit a kick in one dimension and seeing that the oscillation is properly decoupled downstream. Figure 6 shows how a horizontal kick causes an oscillation which is coupled into the vertical by a roll. In Fig. 6a the coupling is eliminated after the compensating roll because the phase error is small. In Fig. 6b, a phase shift error causes residual coupling. By adjusting magnet positions and correction coil excitations, phase shift errors have been corrected in the electron arc. Adjustment has started in the positron arc. Further studies of techniques of phase shift error measurement and of techniques for reducing sensitivity to phase shift errors are continuing. For instance, distributing the roll over several magnets can provide local compensation of coupling; whereas, the coupling is currently compensated at a distant roll allowing more accumulated phase shift error.

Final Focus

The final focus optical system as currently built is designed to produce a 2.4 micron RMS spot size at the interaction point. Future installation of superconducting quadrupoles in the final telescopes will allow further demagnification to 1.6 microns. The final focus is instrumented to guide the small beams into collision and to extract the beams to dumps after collision. It also contains adjustable collimators and masks for reducing backgrounds around the interaction point.

The electron beam has been focused to spot sizes as small as 7.8×6.0 microns. The spot size is measured by scanning a 3.5 micron radius wire across the beam. A typical scan is illustrated in Fig. 7. The wire size contributes to the

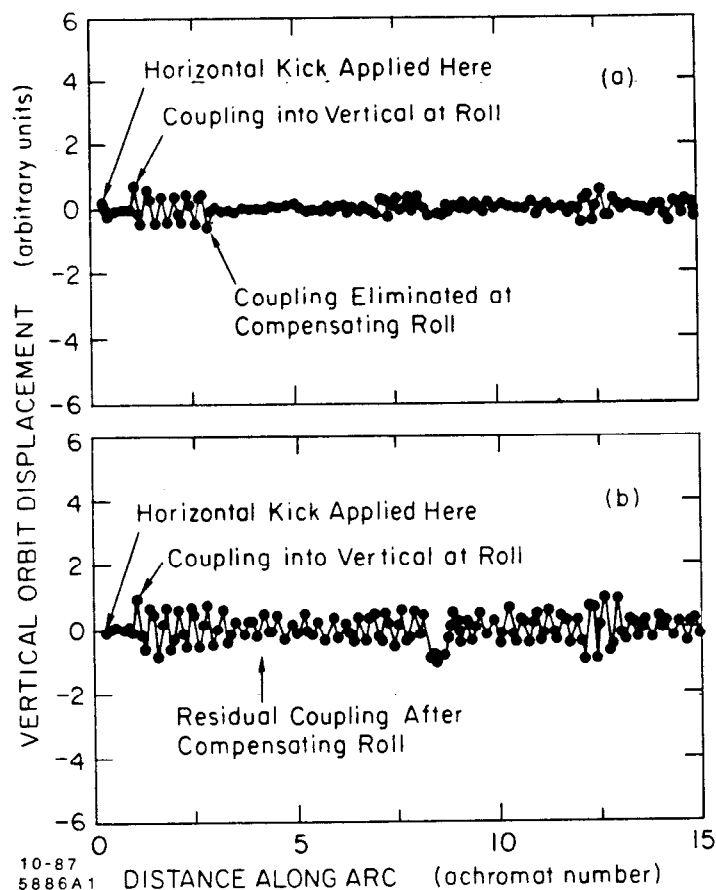


Fig. 6. Vertical beam orbit displacement as a function of distance along the arc for a beam to which a horizontal kick has been applied at the entrance to the arc. The horizontal oscillation couples into the vertical at a magnet roll. If the phase shift error is small, as in (a), the coupling is eliminated at the compensating roll. If a residual phase shift error exists, as in (b), the coupling remains beyond the compensating roll.

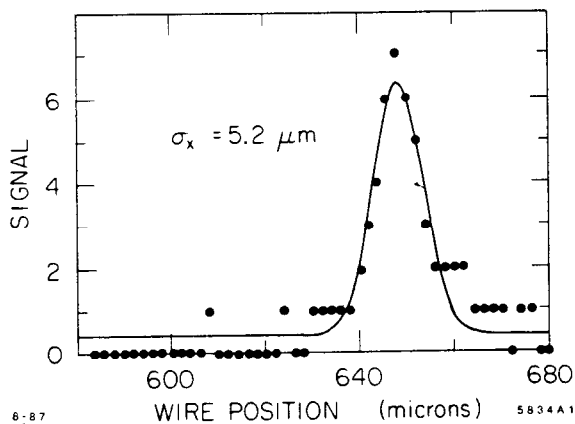


Fig. 7. A horizontal scan of the beam profile near the SLC collision point using a $3.5 \mu\text{m}$ radius wire. Unfolding the contribution due to the wire size gives an RMS beam radius of $4.6 \mu\text{m}$.

measured size, as would any beam jitter during the scan. Spot sizes smaller than five to six microns are not expected without use of the sextupoles, which have not yet been used in these studies.

Although commissioning has concentrated to date on studies of optics with a single beam, two beams were brought into collision for a period of days before the Autumn 1987 shutdown. While both beams were delivered to the interaction point, the longitudinal position of the interaction point was measured to an accuracy better than one millimeter. Knowledge of this location is important in order to focus both beams to the same point.

In order to bring the beams into collision in the presence of the Mark II detector, a new wire target device was commissioned prior to the Autumn 1987 shutdown. With vertical and horizontal 3.5 micron radius wires near the interaction point, the beams can be individually tuned by scanning them across the wire. When the beam profile is smaller than the 3.5 micron wires, it will be scanned across a pair of two micron wires. The wires will then be flipped out of the beam, and the beams can be brought to within ten microns of each other using a vertex beam position monitor which measures the relative position of the beams. The beams will then be centered on each other to within one-quarter of their radii using beam position monitors to measure the deflection of the beams in passing, which disappears when they collide head-on. Finally, the luminosity will be optimized using detectors of the beamstrahlung, or synchrotron radiation emitted by the beams in the fields of the other beam.

Summary Status as of October 1987

Although many aspects of the commissioning of the SLC remain to be accomplished, many important milestones have been passed. At this time, Autumn 1987, the commissioning has been interrupted in order to place the Mark II detector at the collision point and to make improvements to the SLC which will allow better luminosity to be achieved during early physics running. Important improvements currently being incorporated include installation of the electron ring extraction kicker for 120 Hz operation, improvement to the ring-to-linac bunch compression systems for 3×10^{10} particles, repair of damaged components in the positron source for doubling positron yield, and such measures as additional shielding and collimators for reduced radiation effects and backgrounds in the final focus. Other improvements, such as electron polarization, superconducting final-focus quadrupoles for even smaller spot sizes, and higher currents and repetition rates remain for the future.

STATUS OF THE MARK II

Overview

Z^0 physics at the SLC will begin with an upgraded PEP detector, the Mark II, and follow with a new state-of-the-art detector, the SLD. The proposal¹⁾ to upgrade the Mark II for the SLC was approved in November 1982. Design of a new central tracking chamber had begun about a year earlier. All new detector components which could be tested at PEP were built and installed by Summer 1985. These new devices included, in addition to the new chamber, a new room temperature magnet coil, new time-of-flight scintillators and tubes, new endcap shower counters, and a new on-line computer. Mark II ran at PEP for five months from November 1985 to March 1986 and collected 30 pb^{-1} of data. All new detector components met or exceeded their design specifications. The detector was then moved from PEP to the SLC and has been running on cosmic rays since January 1987. The Mark II is being placed on the beam line during the current Autumn 1987 shutdown. New small angle monitors are being installed, and some additional improvements are being prepared.

For the SLC the original Mark II groups from LBL and SLAC have been joined by additional groups from CALTECH, Colorado, Hawaii, Indiana, Johns Hopkins, Michigan, Santa Cruz, and SLAC. A cut-away view of the Mark II detector showing the major components appears in Fig. 8.

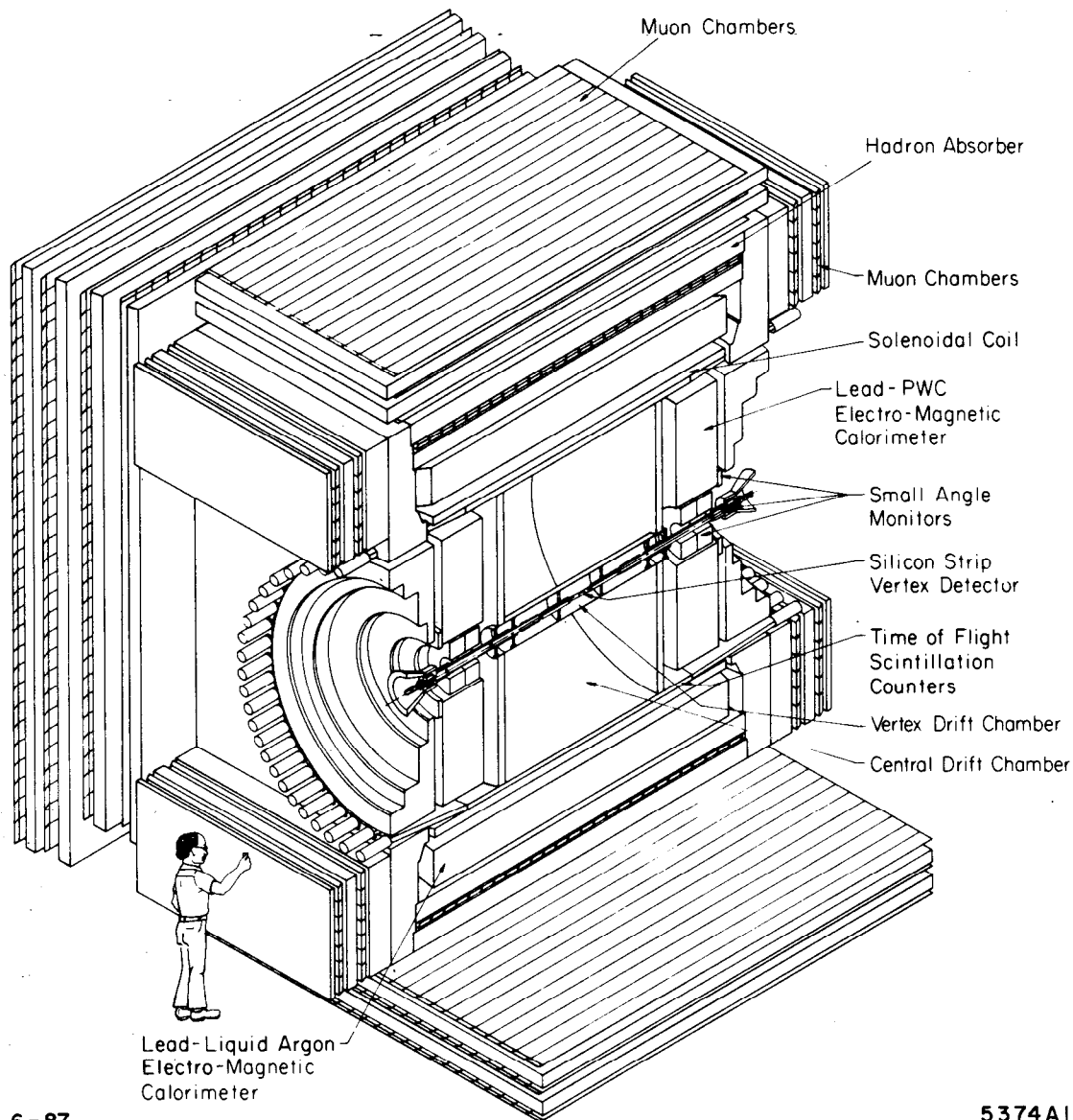
The goal of upgrading the Mark II was to have a thoroughly tested detector ready for physics when luminosity is first available at the SLC. The original Mark II detector, nonetheless, has been substantially improved in several areas: tracking and vertexing, lepton identification, and hermeticity. In addition, spectrometers are being added to the SLC extraction lines in order to precisely measure the beam energies.

Improvements to Tracking and Vertexing

Tracking has been improved by the addition of the new central drift chamber.²⁾ It provides improved pattern recognition using minijet cells and can measure double hits separated by about three millimeters. Momentum resolution with a vertex constraint is $\sigma/p = 0.15\%p$, and the chamber provides coverage for $|\cos \theta| \leq 0.90$.

Vertexing will be provided by two detector systems now in fabrication and to be installed around Summer 1988. These systems exploit the small diameter SLC beam pipe for excellent impact parameter resolution. The first system is a drift chamber vertex detector³⁾ shown schematically in Fig. 9. It consists of ten canted jet cells of 38 sense wires each between radii of five and fifteen centimeters.

MARK II AT SLC



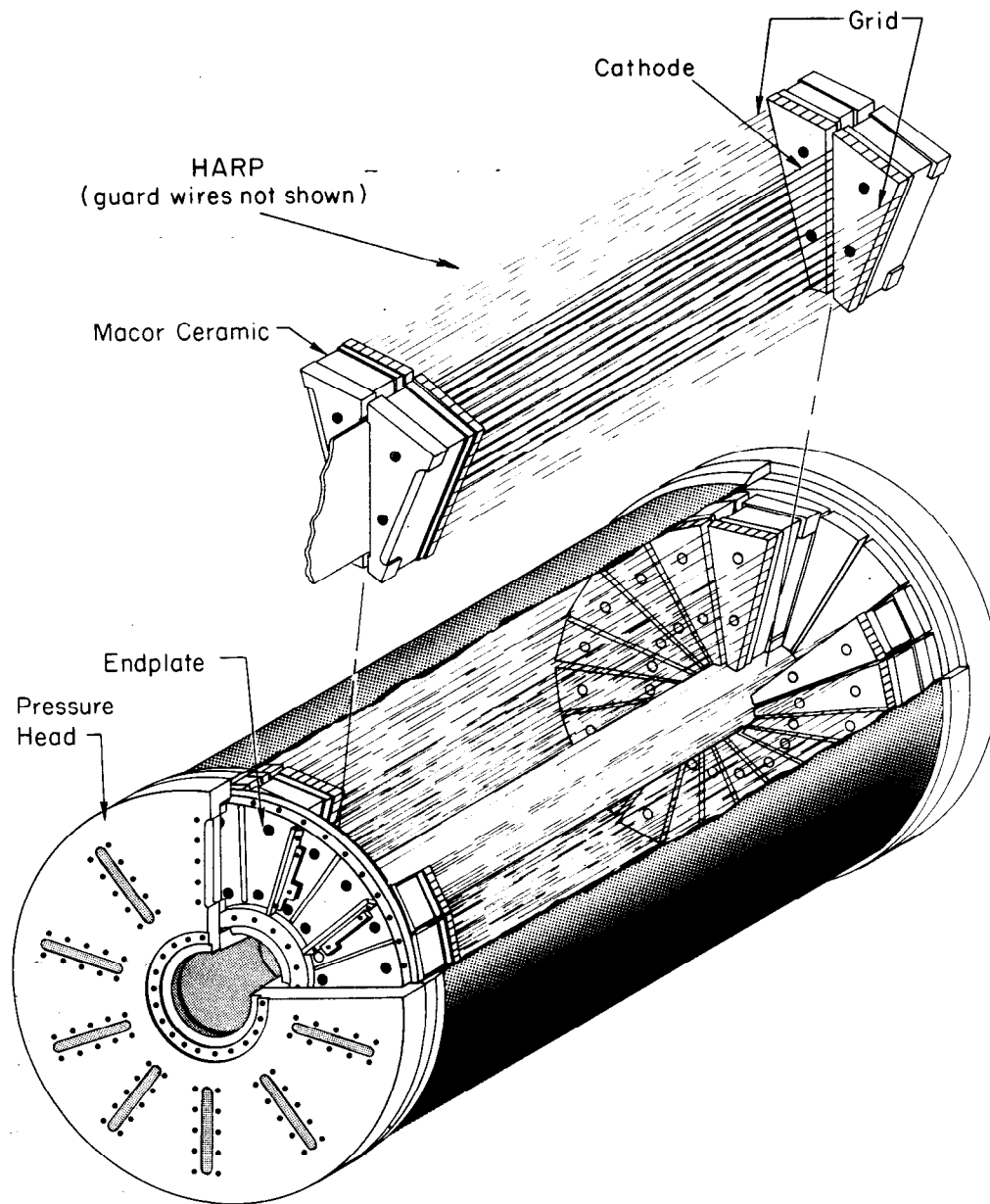
6-87

5374A1

Fig. 8. Cut-away view of the Mark II detector.

Wires are positioned on high-precision machined ceramic. Planes of grid wires surround the sense wire plane in order to provide more isochronous arrival of drift electrons. The chamber will be operated at three atmospheres pressure with a gas having slow drift velocity ($7 \mu\text{m}/\text{nsec}$). Its design concentrates on good two-track separation and on excellent impact parameter resolution ($20 \mu\text{m} + 75 \mu\text{m}/p$).

The second vertex detector system consists of three layers of three to four centimeter long silicon microstrips.⁴⁾ A detector assembly is shown in Fig. 10. Readout of the microstrips is via a custom VLSI circuit which permits this type of



DRIFT CHAMBER VERTEX DETECTOR

7-85

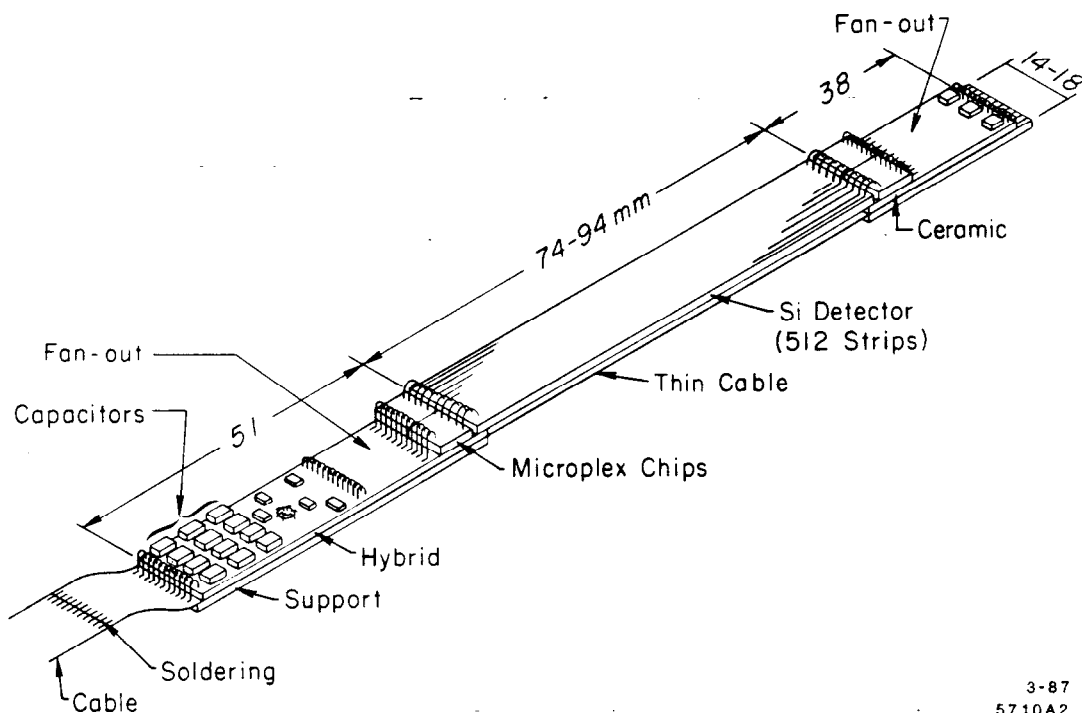
5184B1

Fig. 9. Cut-away view of the Mark II drift chamber vertex detector, showing modular construction.

detector to be used in a cylindrical geometry for the first time. Position resolutions of 3.5 microns are achieved, and impact parameter resolution of $5 \mu\text{m} + 15 \mu\text{m}/p$ is expected.

Improvements to Lepton Identification

Electron identification in the Mark II has been improved by dE/dx measurement in the central drift chamber complemented by the improved time-of-flight system and by the new endcap shower counters.



3-87
5710A2

Fig. 10. A silicon microstrip assembly for the Mark II silicon strip vertex detector.

The dE/dx measurement is provided by seventy-two 8.3 mm samples in 89% Ar/10% CO₂/1% CH₄ gas. The measured resolution is $(7.0 \pm 0.1)\%$, and electrons are separated from pions by more than two sigma to momenta greater than 10 GeV. Figure 11 shows the dE/dx signals observed for samples of pions from multihadronic events and electrons from photon conversions and QED events. Note the electron contamination in the time-of-flight selected pion sample which is visible in the electron region of dE/dx .

The endcap shower counters cover the polar angle region between the liquid argon shower counters in the barrel region and $|\cos \theta| = 0.96$. They have a four-view strip geometry which gives good π/e separation in multiparticle events with modest channel count. There are four longitudinal segments. Construction is of proportional tubes and lead.

Muon identification will be improved by extending the solid angle coverage into the forward region. "Facades" of lead, iron, and drift tubes are being added above and below the endcaps at each end of the detector. Muon coverage is improved by about 30%. Coverage in the forward region will play an important role in studying $Z^0 \rightarrow \tau^+\tau^-$. The improved muon and electron coverage will also significantly increase samples of multileptonic events, such as decays of heavy quark pairs.

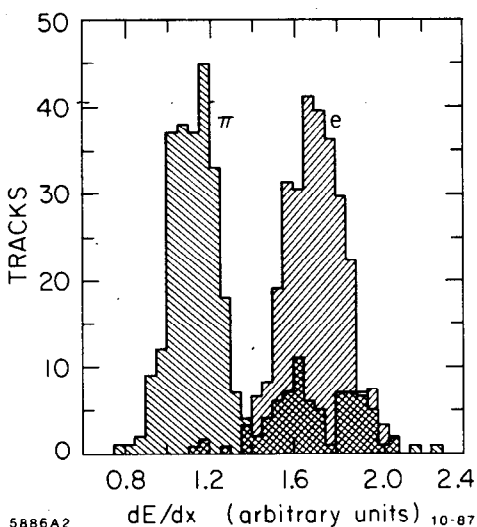


Fig. 11. Histogram of dE/dx signals for a sample of electrons and a sample of pions from multihadronic events at PEP. Note that the time-of-flight selected pion sample has some electron contamination.

Improvements to Hermeticity

Hermeticity of the Mark II detector is improved by the addition of the new small angle monitors, which consist of nine layers of drift tubes followed by a lead/proportional tube calorimeter. The angular regions between the small angle monitors and the endcaps are covered by an annular veto counter composed of lead and scintillator. Angles smaller than the small angle monitors are covered by tungsten/scintillator mini-small angle monitors and by beam line masks instrumented with scintillator. The cracks between liquid argon modules in the barrel region are also covered by lead/scintillator veto counters. The greatly improved hermeticity will be useful to $Z^0 \rightarrow \gamma\nu\bar{\nu}$ experiments and supersymmetry searches.

Energy Spectrometers

In order to make precision measurements of the parameters of the Z^0 resonance, an energy spectrometer is being installed in each extraction line transporting beam from the collision point to a dump. A spectrometer, shown very schematically in Fig. 12, consists of a large vertical bend between two small horizontal bends. The horizontal bends produce very intense swathes of synchrotron radiation photons which are imaged onto synchrotron light monitors. The measured displacement between the bands of synchrotron radiation, provided by the vertical spectrometer bend, determines the beam energy. A precision measurement of the bending field is provided by laboratory calibration with an accuracy of about 10^{-5} and in situ monitoring to 3×10^{-5} .

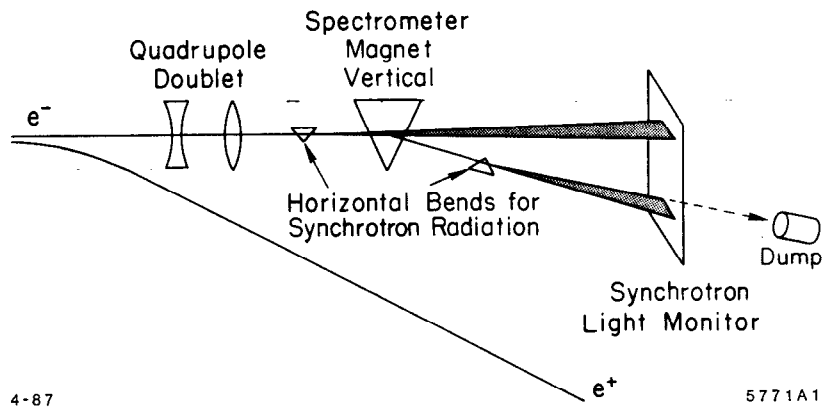


Fig. 12. Conceptual view of an energy spectrometer in an SLC extraction line.

Two synchrotron light monitors will exist in each spectrometer. The first is a phosphorescent screen monitor viewed by a vidicon camera whose output is digitized. The second is a detector consisting of finely spaced wires upon which photons Compton scatter. Electrons ejected from the wires provide signals on the wires proportional to the distribution of illumination. The wires are $75 \mu\text{m}$ diameter copper on $100 \mu\text{m}$ centers. Both detectors are expected to find the centroid of each synchrotron radiation band to 75 microns, compared to the 27 centimeter displacement. The wire detector will allow measurement of the beam energy for every SLC pulse.

By controlling the systematics of magnetic measurement and of alignment, the accuracy of the energy measurement will be dominated by the measurement of the synchrotron light and perhaps by unforeseen beam dispersion at the collision point. The absolute accuracy of the center-of-mass energy measurement will be 45 MeV. The pulse-to-pulse accuracy will be 35 MeV. This accuracy will yield a measurement of the Z^0 mass to 45 MeV with only 3000 events. Such a measurement is equivalent to an error in $\sin^2 \theta_W$ of 0.00030. The same data sample will measure the width of the Z^0 resonance to 134 MeV; whereas, the ultimate accuracy on the width will be about 35 MeV, determined by the pulse-to-pulse accuracy. The pulse-to-pulse accuracy will also be important to measuring forward-backward asymmetry. Ultimately, the value of $\sin^2 \theta_W$ deduced from the mass measurement will be compared to a comparably accurate measurement of the polarization asymmetry to provide a stringent test of the Standard Model.

Both energy spectrometers are being installed during the Autumn 1987 shut-down and will be operational for the first physics running.

Preparations for Physics at SLC

In preparing for physics at the SLC, the 30 pb⁻¹ data sample recorded at PEP has been used to tune the detector and the tracking and analysis programs. Three physics publications have resulted. A new measurement of the D^0 lifetime⁵⁾ exploited the improved momentum resolution to extract a clean $D^{*+} \rightarrow D^0 \pi^+ \rightarrow K^-(n\pi)^+ \pi^+$ signal with small statistics. A study of energy-energy correlations,⁶⁾ which is dominated by systematics, was improved by the excellent two-track separation and by the greater solid angle coverage. Finally, a study of multihadronic event parameters⁷⁾ provided an opportunity to tune the understanding of the detector with regard to acceptance and efficiencies, as well as to tune the Monte Carlo generators which will be used in physics at the SLC. The experience gained during the PEP run will significantly reduce the time between the first luminosity and the production of quality data for analysis.

In addition, considerable preparation for SLC physics has occurred in a number of Mark II physics study groups and workshops.⁸⁾ Particular effort has been invested in understanding electroweak radiative corrections and in distinguishing the signals of various potential sources of new physics. These studies also pointed out the need for many of the improvements now being made to the Mark II.

CONCLUSION

In November 1987, commissioning of the SLC will resume for systems upstream of the end of the linac. By the end of 1987, installation work will be complete in the final focus region and commissioning of the complete SLC with the Mark II on the beam line will continue. It is anticipated that a physics run will start when luminosity reaches 6×10^{27} cm⁻² sec⁻¹ and Z^0 production is about 15 per day. Luminosities will increase as commissioning continues.

ACKNOWLEDGEMENTS

This status report drew heavily upon previous talks given by Rae Stiening⁹⁾ at Washington in March 1987 and by Burton Richter¹⁰⁾ at Hamburg in July 1987. I also appreciate the help of Witold Kozanecki and John Seeman in preparing this report. The work reported upon here is being performed by a large group of individuals, too many to acknowledge individually.

REFERENCES

1. Trilling, G. *et al.*, SLAC-PUB-3561 (1983).
2. Hanson, G., Nucl. Instrum. Methods A252, 343 (1986).

3. Hayes, K. G., SLAC-PUB-4255 (1987), to be published in the Proc. of the Int. Conf. on Advances in Experimental Methods for Colliding Beam Physics, Stanford, CA (1987).
4. Litke, A. *et al.*, SLAC-PUB-4400 (1987), to be published in the Proc. of the Int. Conf. on Advances in Experimental Methods for Colliding Beam Physics, Stanford, CA (1987).
5. Wagner, S. R., *et al.*, SLAC-PUB-4304, (1987), submitted to Phys. Rev. D.
6. Wood, D. R., *et al.*, SLAC-PUB-4374 (1987), to be submitted to Phys. Rev. D.
7. Petersen, A. *et al.*, SLAC-PUB-4290 (1987), Submitted to Phys. Rev. D.
8. Proc. of the Second Mark II Workshop on SLC Physics, Tahoe City, CA, [SLAC-0306] (1986).
9. Stiening, R., SLAC-PUB-4263 (1987), to be published in Proc. of the 12th Particle Accelerator Conf., Washington, D.C. (1987).
10. Richter, B., and Stiening, R., SLAC-PUB-4367 (1987), to be published in Proc. of the Int. Symp. on Lepton and Photon Interactions at High Energies, Hamburg, Germany (1987).